

NON-EQUILIBRIUM AND COLLECTIVE FLOW EFFECTS IN RELATIVISTIC HEAVY ION COLLISIONS

T. GAITANOS, H.H. WOLTER
*Sektion Physik der Universität München
Am Coulombwall 1, D-85748 Garching, Germany*

AND

C. FUCHS
*Institut für Theoretische Physik der Universität Tübingen
Auf der Morgenstelle 14, Tübingen, Germany*

1. Introduction

Heavy ion physics opens the unique opportunity to explore the nuclear equation of state (EOS) far away from saturation, i.e. at high densities and at non zero temperatures. Investigations of nuclear matter under such extreme conditions are crucial for the understanding of the universe, its evolution and the formation of the elements, and the evolution of massive stars, supernovae and neutron stars.

The intensive study of heavy ion collisions has become possible by the introduction of new generations of accelerators and detectors, which allow to study collisions of heavy nuclei from Fermi energies up to high relativistic energies of a few hundred GeV per nucleon with an almost complete characterization of the reaction products of the space-time events.

In spite of the theoretical efforts over the last three decades (see ref. [1]) the determination of the EOS in heavy ion reactions is still an object of current debate. Comparisons with experiments seem to favor a nuclear EOS with an incompressibility of $K \approx 230 MeV$ and with a moderate density dependence at high densities (soft EOS). In particular, a difficulty in the determination of the nuclear EOS is the fact that the nuclear matter is to a large extent far away from local equilibrium in a heavy ion collision. These non-equilibrium effects are a main feature of energetic nuclear collisions, and govern the dynamics of the reaction with relaxation times comparable to the compression phase of the process [2]. These effects originate from

an anisotropy in momentum space and lead to effective fields which are different from the ground state [3].

In this contribution we discuss the origin of non-equilibrium features, their influence on the nuclear matter EOS and the consequences when drawing conclusions on the nuclear EOS from comparisons with experiments in terms of collective flow effects.

2. The nuclear EOS: from nuclear matter to heavy ion collisions

The theoretical concept of the description of nuclear matter (NM) is given in an effective relativistic quantum field theory, Quantumhadrodynamics (QHD) [4]. It is formulated in terms of baryon and meson fields as the important non-perturbative degrees of freedom of QCD. A relativistic treatment is attractive since it yields a natural description of characteristic features of NM, such as the appearance of strong attractive scalar and repulsive vector fields which naturally account for the saturation mechanism and for the strong spin-orbit potential. Relativity also leads to effectively energy dependent fields, which are crucial for nucleon-nucleus reactions and also heavy ion collisions. The effective Lagrangian of QHD involving baryon and meson fields is given by (for brevity, only scalar σ and vector ω^μ meson fields are considered here)

$$\begin{aligned}
\mathcal{L}_{QHD} &= \mathcal{L}_B + \mathcal{L}_M + \mathcal{L}_{int} \\
\mathcal{L}_B &= \bar{\Psi}(i\gamma_\mu\partial^\mu - M)\Psi \\
\mathcal{L}_M &= \frac{1}{2}\left(\partial_\mu\sigma\partial^\mu\sigma - m_\sigma^2\sigma^2\right) - \frac{1}{4}F_{\mu\nu}F^{\mu\nu} - m_\omega^2\omega_\alpha\omega^\alpha \\
\mathcal{L}_{int} &= \Gamma_\sigma\bar{\Psi}\Psi\sigma - \Gamma_\omega\bar{\Psi}\gamma_\alpha\Psi\omega^\alpha \quad ,
\end{aligned} \tag{1}$$

with $F^{\mu\nu} = \partial^\mu\omega^\nu - \partial^\nu\omega^\mu$ the field tensor. The mesons σ and vector ω^μ are coupled in a minimal way to the nucleons via effective couplings Γ_σ and Γ_ω , respectively.

Different approximations have been used for the solution of eq. (1) in nuclear matter. The most popular one is the Hartree or Relativistic Mean Field (RMF) approach where the meson fields are treated classically [4]. A more realistic treatment is the Dirac-Brueckner-Hartree-Fock (DBHF) theory, in which exchange terms and higher order correlations within a \mathcal{T} -Matrix or ladder approximation are taken into account [5]. The success of DBHF theory was in the unified description of nucleon-nucleon (NN) scattering and saturation properties of nuclear matter which was not possible in non-relativistic approaches, except by including 3-body forces. The nucleonic mean field potential is given in terms of self energies by

$$\Sigma^{DBHF}(p, p_F) = \Sigma_s(p, p_F) - \gamma_\mu\Sigma^\mu(p, p_F) \quad , \tag{2}$$

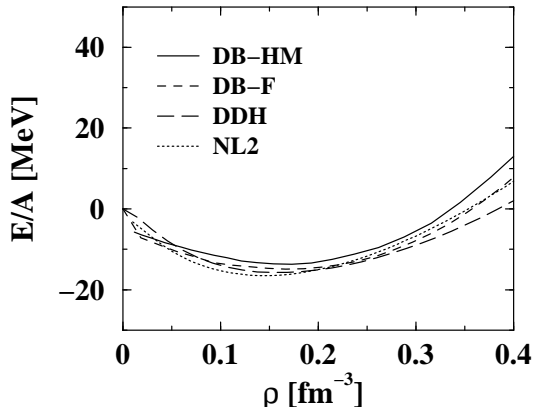


Figure 1. Nuclear matter EOS for different models: (solid) DBHF from [8], (dashed) DBHF from [9], (long-dashed) RMF with density dependent couplings [10] and (dotted) Walecka model (NL2 parametrization) [11]

with scalar and vector components Σ_s, Σ^μ depending on density $\rho(p_F)$ and for energies higher than the Fermi energy on momentum p . For NM the DBHF theory is parameter free, since it is based on a model for the bare NN interaction given by boson exchange potentials [6]. This is in contrast to phenomenological approaches, where several parameters are adjusted to NM saturation properties.

The application of DBHF theory to finite nuclei has been formulated in a Density Dependent Hadronic (DDH) field theory [7], where the self energies are parametrized in Hartree form by

$$\Sigma_s = \Gamma_s(p, p_F) \rho_s(p_F) \quad , \quad \Sigma_\mu = \Gamma_0(p, p_F) j_\mu \quad , \quad (3)$$

with density and momentum dependent vertex functions $\Gamma_{s,0}$ that replace the constant values of the RMF approach ($\Gamma_{s,0} \rightarrow \Gamma_{\sigma,\omega}^2/m_{\sigma,\omega}^2$). They effectively contain exchange and correlation effects of the DBHF theory. Fig. 1 compares the density dependence of the ground state EOS obtained from different models, which show a similar density behavior around saturation, but significant differences at high densities. The density dependence of the EOS at supra-normal densities can be regarded as an extrapolation which is tested in heavy ion collisions, where high compressions of the matter are reached.

However, the determination of the nuclear matter EOS from heavy ion collisions is only indirect, because it contains fields corresponding to non-equilibrium colliding matter. Thus one does not, in fact, see the equilibrated nuclear matter EOS directly in heavy ion collisions.

Equilibrated nuclear matter is characterized by an isotropic spherical momentum distribution. This is not the case in the dynamical situations

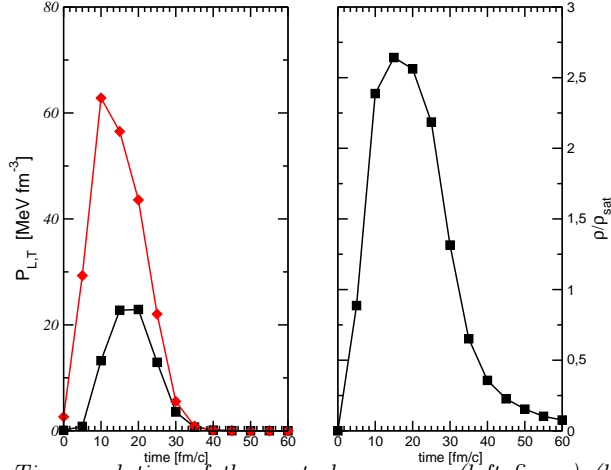


Figure 2. Time evolution of the central pressures (left figure) (longitudinal P_L and transversal P_T) and the central density (right figure) for a central Au + Au heavy ion collision at $E_{\text{lab}} = 0.4$ A.GeV

of heavy ion collisions. This is seen in Fig. 2 in terms of the transversal and longitudinal components of the *local* central pressure, obtained in calculations with a transport equation, as described in the next section. The anisotropy in the pressure components indicates that the matter is *locally* not equilibrated, except at the late stage of the process ($t > 30$ fm/c). Indeed, the relaxation times are large and comparable with the compression phase of the collision (see time evolution of the central density in 2). Therefore, it is important to first study possible influences of phase space anisotropies on the nuclear matter EOS before making comparisons with experiments.

The investigation of non-equilibrium effects on the level of the effective mean fields has been done by considering two models: a Local Density and a Colliding Nuclear Matter approximations, denoted as LDA and CNM respectively. In the LDA the EOS and the corresponding fields are those of equilibrated matter described by an isotropic momentum distribution. The mean field $\Sigma(p_F, p) = \Sigma_s(p_F, p) - \gamma_\mu \Sigma^\mu(p_F, p)$ depends on a density $\rho(E_F)$ and for energies above the Fermi energy E_F on momentum p relative to the rest system of nuclear matter. The density dependence has been taken from phenomenological (Walecka, DDH) or microscopic (DBHF) models. The momentum dependence is also naturally provided from the DBHF theory, whereas in the DDH approach it has been adjusted to the energy dependence of the Schrödinger equivalent optical potential in nucleon-nucleus scattering [12]. The fields of the non-linear Walecka model (NL2) do not depend on energy.

In the CNM model the anisotropy of momentum space is modeled by

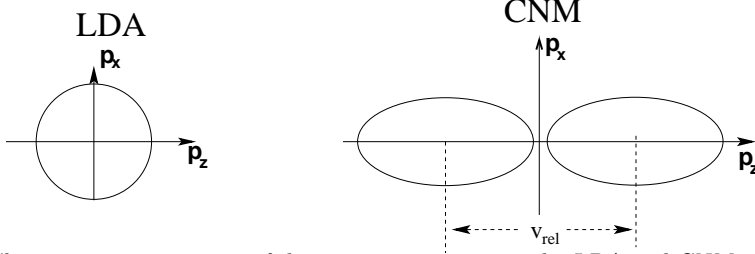


Figure 3. Schematic representation of the momentum space in the LDA and CNM models.

that of two covariant Fermi-ellipsoids, i.e. two interpenetrating currents of nuclear matter (see Fig. 3) $f_{CNM}(p_{F_1}, p_{F_2}, v_{rel}) = f_1(p_{F_1}) + f_2(p_{F_2}) + \delta f(p_{F_{1,2}}, v_{rel})$ where the last term takes Pauli effects into account. This representation of phase space anisotropies is motivated from microscopic calculations of heavy ion collisions [13]. The mean field is then given (e.g. for the scalar part) approximately by

$$\Sigma^{CNM}(p, p_F; v_{rel}) = \Sigma_{s1}(\Lambda_1^{-1}p, p_{F_1}) + \Sigma_{s2}(\Lambda_2^{-1}p, p_{F_2}) + \delta\Sigma(\Lambda_{1,2}^{-1}p, p_{F_{1,2}}, v_{rel}) \quad , \quad (4)$$

i.e. as a superposition of self energies of the nucleon with respect to the two currents taking into account the Lorentz transformations $\Lambda_{1,2}$ for the momenta and the Pauli correction in the overlap region ($\delta\Sigma$). This ensures the correct limit to the LDA of one Fermi-sphere, i.e. $CNM \xrightarrow{v_{rel} \rightarrow 0} LDA$. As a further approximation an average of the p -dependent quantities $\Sigma_{s,0,v,\dots}^{CNM}$ over the CNM configuration leads to fields depending only on the configuration parameters, i.e. the two Fermi momenta $p_{F_{1,2}}$ and the relative velocity v_{rel} [14].

The energy-momentum tensor $T^{\mu\nu}$ is given in terms of the CNM fields by [3, 14]

$$\begin{aligned} T^{\mu\nu} &= \langle p^{*\mu} p^{*\nu} / E^* \rangle_{CNM} - \langle p^{*\mu} \Sigma^{CNM\nu} / E^* \rangle_{CNM} \\ &- \frac{1}{2} g^{\mu\nu} \left[\langle \Sigma_s m^* / E^* \rangle_{CNM} - \langle p^{*\lambda} \Sigma_\lambda^{CNM} / E^* \rangle_{CNM} \right] \quad , (5) \end{aligned}$$

where $\langle \dots \rangle_{CNM}$ means the average over the CNM momentum space. The energy per nucleon $E^{CNM}(\rho_{tot}, v_{rel}) = T^{00} / \rho_{tot} - M$ depends on the total invariant density $\rho_{tot} = \sqrt{j_{tot\alpha} j_{tot}^\alpha}$ and the relative velocity v_{rel} . However, the total energy E^{CNM} contains contributions from the energy of the relative motion of the two currents. A meaningful discussion of non-equilibrium effects with respect to the ground state EOS should be based on the binding energy and thus it is reasonable to subtract contributions from the relative motion of the two currents E_{rel} . E_{rel} can be relativistically defined as the difference of the kinetic energy of the CNM system and the

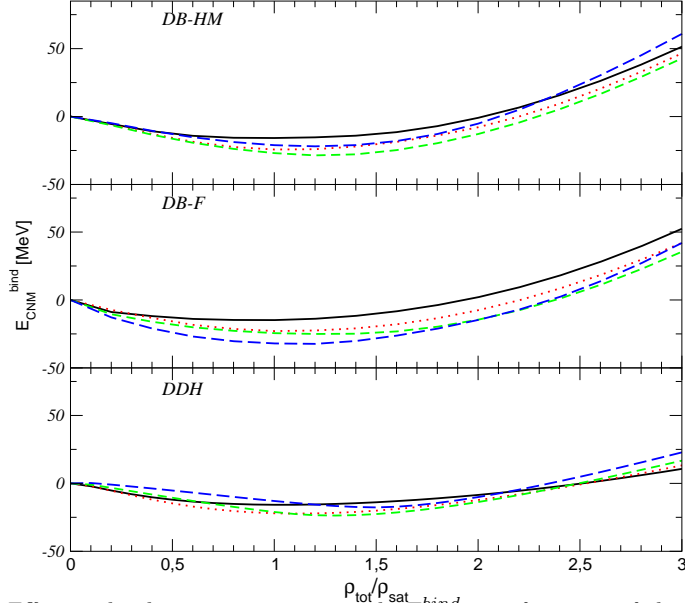


Figure 4. Effective binding energy per particle E_{CNM}^{bind} as function of the total density ρ_{tot} (normalized to the saturation density ρ_{sat}) at different relative velocities v_{rel} (solid: $v_{rel} = 0$, dotted: $v_{rel} = 0.2$, dashed: $v_{rel} = 0.4$ and long-dashed: $v_{rel} = 0.6$) for the DBHF theory from Refs. [8] (DB-HM) and [9] (DB-F) and for the DDH approach [10].

corresponding LDA configuration at twice the subsystem density 2ρ

$$E_{rel}(\rho_{tot}, v_{rel}) = \langle \sqrt{p^{*2} + m^{*2}} - m^* \rangle_{CNM} - \langle \sqrt{p^{*2} + m^{*2}} - m^* \rangle_{v_{rel}=0} \quad (6)$$

By definition E_{rel} contains the kinetic energy arising from the separation of the Fermi-spheres in momentum space. It accounts for the interaction between the two currents by the presence of the effective mass in eq. (6). One should note that eq. (6) is the natural definition of a relativistic kinetic energy of the relative motion of two *interacting* currents and contains, in particular, the correct non-relativistic limit [3].

Now one is able to construct an effective bound energy of colliding nuclear matter $E_{CNM}^{bind}(\rho_{tot}, v_{rel})$

$$E_{CNM}^{bind}(\rho_{tot}, v_{rel}) = \frac{T^{00} - E_{rel}}{\rho_{tot}} - M \quad , \quad (7)$$

which relates colliding to ground state nuclear matter. E_{CNM}^{bind} is displayed in Fig. 4 for different models. The case $v_{rel} = 0$ is the correct limit for LDA. With increasing v_{rel} we observe a *softening of the effective EOS* in

terms of an increase of the binding energy at $\rho_{tot} \sim \rho_{sat}$ and a decrease of E_{CNM}^{bind} at high densities ($\rho_{tot} \gg \rho_{sat}$) with respect to the ground state EOS (solid curves in Fig. 4). The softening of the effective EOS occurs in all the models investigated and can be explained by (a) a decrease of the fields $\Sigma_{s,0,v,\dots}^{CNM}$ with density and momentum, see eq. (4), (b) a reduction of the Fermi pressure (not shown here) in transverse direction and (c) an enlarged scalar attraction with increasing relative velocity [3]. It is important that the differences between the non-equilibrium and the ground state EOS are of the same magnitude as the differences of the ground state EOS for different models, see e.g. Fig. 1. Thus we conclude that one should take non-equilibrium effects into account when determining the EOS in heavy ion collisions. In the next section we investigate the non-equilibrium effects in transport calculations of heavy ion collisions in terms of collective flow observables.

3. Heavy ion collisions

Heavy ion collisions have been described by covariant transport equations of a Boltzmann type (details can be found in refs. [11, 15]):

$$\begin{aligned}
& \left[(m^* \partial_x^\mu m^* - p^{*\nu} \partial_x^\mu p_\nu^*) \partial_\mu^p - (m^* \partial_p^\mu m^* - p^{*\nu} \partial_p^\mu p_\nu^*) \partial_\mu^x \right] f(x, \mathbf{p}) \\
&= \frac{1}{2} \int \frac{d^4 p_2}{E_{p_2}^* (2\pi)^3} \frac{d^4 p_3}{E_{p_3}^* (2\pi)^3} \frac{d^4 p_4}{E_{p_4}^* (2\pi)^3} W(pp_2|p_3p_4) (2\pi)^4 \delta^4(p + p_2 - p_3 - p_4) \\
&\times \left[f(x, \mathbf{p}_3) f(x, \mathbf{p}_4) (1 - f(x, \mathbf{p})) (1 - f(x, \mathbf{p}_2)) - \right. \\
&\quad \left. f(x, \mathbf{p}) f(x, \mathbf{p}_2) (1 - f(x, \mathbf{p}_3)) (1 - f(x, \mathbf{p}_4)) \right] , \tag{8}
\end{aligned}$$

with effective quantities $p^{*\mu} = p^\mu - \Sigma^\mu$ and $m^* = M - \Sigma_s$. It describes the evolution of the phase space density $f(x, p)$ under the influence of a mean field in the left hand side of eq. (8) and on the right hand side of 2-body collisions determined by energy and isospin dependent NN-cross sections $\sigma_{NN} \sim W(pp_2|p_3p_4)$ for the process $p + p_2 \rightarrow p_3 + p_4$. The Pauli principle is taken into account for the final states by the terms $(1 - f)$. The NN-cross section is taken from empirical NN-scattering data. Also inelastic channels are taken into account as the production of Δ and N^* resonances with their decay in 1- and 2-pion channels [2, 16]. The EOS enters into the theoretical descriptions of heavy ion reactions via the self energies.

We have applied the approximations discussed in the previous section, the LDA and CNM approaches, in transport calculations using eq. (8). In the LDA model the ground state EOS enters directly into the transport equation neglecting non-equilibrium effects, whereas in the CNM model the effective EOS including the momentum space anisotropies is consid-

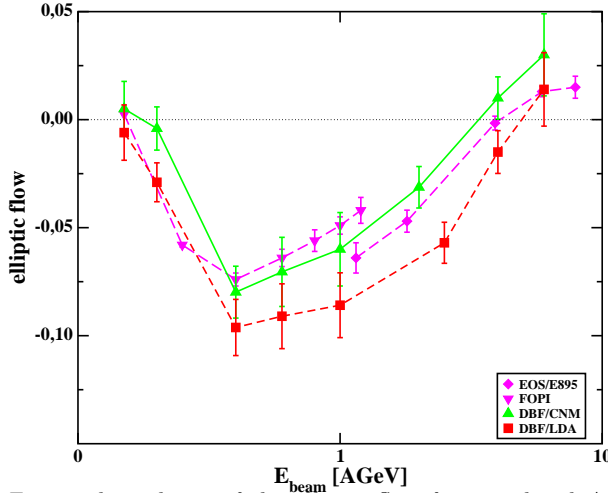


Figure 5. Energy dependence of the elliptic flow for peripheral $Au + Au$ collisions at energies from the Fermi energy to AGS energies. Calculations with the DBHF model [9] are shown in the LDA and CNM approximations and compared to data [17].

ered in eq. (8). In the latter case the CNM parameters, i.e. the invariants ρ_1 , ρ_2 , v_{rel} , are determined directly from the phase space density $f(x, p)$ at each position and in each time step of the simulation.

We discuss the results of transport simulations in terms of collective flows, which have been found to be sensitive to the density and, particularly, momentum dependence of the mean field [18]. The collective flow is characterized by a Fourier series of the azimuthal distribution of nucleons for given rapidity y and total transverse momentum p_t , $N(\phi, y, p_t) = N_0(1 + v_1 \cos\phi + v_2 \cos 2\phi \dots)$, where v_1 and v_2 are called transverse and elliptic flow, respectively. As an example, Fig. 5 shows the energy dependence of the elliptic flow at mid-rapidity ($|\Delta y| \leq 0.15$) for peripheral $Au + Au$ collisions. With the cut in the rapidity $y = \frac{E+p_z}{E-p_z}$ one selects particles from the hot and compressed matter in the central region of the reaction, from which one intends to extract information on the nuclear EOS. Thus the elliptic flow describes the dynamics of the compressed *fireball* perpendicular to the beam direction. It probes the high density behavior of the nucleonic fields, i.e. their stiffness, which gives rise to a squeeze-out of the compressed matter perpendicular to the beam direction. An enhancement of the elliptic flow is correlated to a stiffer EOS. The calculations in Fig. 5 were performed with one of the models of the previous section, i.e. the DBHF results of the Tübingen group [9] treated in the LDA and in the CNM approximations. The two different treatments *which are based on identical nuclear forces for ground state matter* yield significantly different results for the elliptic flow.

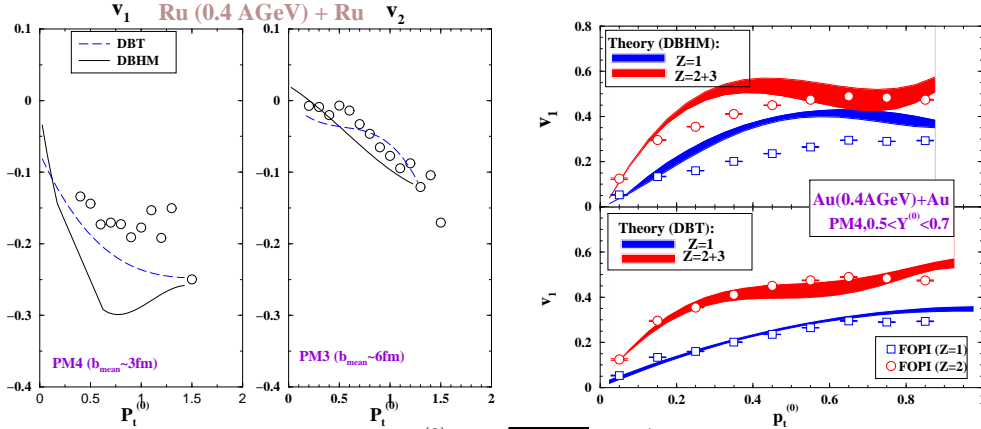


Figure 6. Transverse momentum ($p_t^{(0)} = \sqrt{p_x^2 + p_y^2}/p_t^{proj}$) dependence of the collective flow projected in (v_1) and out of (v_2) the reaction plane. (Left) Comparisons for Ru + Ru and (right) for Au + Au collisions at 0.4 A.GeV beam energy. The figure on the right shows the quantity v_1 for protons ($Z = 1$) and fragments ($Z = 2$). The data (symbols) are from ref. [17] and the theoretical calculations were performed within the DBHF theory of refs. [9, 8] in the CNM model.

Since this observable is particularly sensitive to the EOS at high densities [19, 18], these effects are most pronounced here. In the LDA approach one would have excluded the underlying EOS from the comparison to data as too stiff. The more consistent treatment of momentum space anisotropies on the level of the effective interaction leads to the net softening of the effective EOS discussed above and restores the agreement with experimental data. Similar effects are observed for other models, e.g. those of the previous section, and other components of collective flow not shown here [2, 16].

Other examples of collective flow effects are shown in Fig. 6 with respect to the transverse momentum dependence $p_t^{(0)}$. High $p_t^{(0)}$ -values correspond to highly energetic particles originating from the compressed matter in an early stage of the reaction and thus directly carry information about the high density behavior of the EOS. The DBT calculations with a relatively soft EOS also yield a smoother $p_t^{(0)}$ -dependence of the collective flows closer to the data than the DBHM calculations. This effect, which is observed also for other energies, is consistent with Figs. 4 and 5 indicating that a moderate dependence of the nuclear matter EOS at high densities seems more realistic (similar effects have been found with the phenomenological DDH model).

4. Conclusions

The early and high density phases of relativistic heavy ion collisions are to a large extent governed by highly anisotropic phase space configurations far from local equilibrium, which can be approximated by counter-streaming or colliding nuclear matter configurations. In this contribution we discussed the implications for the effective EOS which occurs in such non-equilibrium configurations and found them to be important. The anisotropy in momentum space leads to a softening of the non-equilibrium EOS with essential deviations compared to the ground state EOS. CNM calculations with different effective interactions for the mean field have shown the general features of this effect. In calculations of energetic heavy ion collisions, where the mean field were considered in the local density (LDA) and in the more realistic CNM approximations, the effective softening of the non-equilibrium EOS was observable in terms of collective flow effects. The differences in the flow signals are found to be comparable to those of the nuclear matter EOS for different models. We conclude that for a reliable determination of the nuclear matter equation of state from heavy ion collisions the non-equilibrium features of the phase space must be taken into account on the level of the effective fields. The results seem to be consistent with a moderate dependence on momentum of the nuclear matter EOS at high densities. With the successful applications of microscopic models to nuclear matter, finite nuclei and heavy ion collisions one expects to move towards a unification of the description of very different nuclear systems and to a determination of the EOS of nuclear matter.

References

1. N. Herrmann, J.P. Wessels, T. Wienold, *Annu. Rev. Nucl. Part. Sci.* **49** (1999) 581.
2. T. Gaitanos, C. Fuchs, H.H. Wolter, *Nucl. Phys.* **A650** (1999) 97.
3. C. Fuchs, T. Gaitanos, submitted for publication.
4. B.D. Serot, J.D. Walecka, *Int. J. Mod. Phys.* **E6** (1997) 515;
P. Ring, *Prog. Part. Nucl. Phys.* **78** (1996) 193.
5. G.J. Horowitz, B.D. Serot, *Nucl. Phys.* **A464** (1987) 613.
6. R. Machleidt, *Advances in Nuclear Physics* **19** (1989) 189.
7. C. Fuchs, H. Lenske, H.H. Wolter, *Phys. Rev.* **C52** (1995) 3043.
8. B. ter Haar, R. Malfliet, *Phys. Rep.* **149** (1987) 207.
9. T. Gross-Boelting, C. Fuchs, A. Faessler, *Nucl. Phys.* **A648** (1999) 105.
10. S. Typel, H.H. Wolter, *Nucl. Phys.* **A656** (1999) 331.
11. B. Blättel, V. Koch, U. Mosel, *Rep. Prog. Phys.* **56** (1993) 1.
12. S. Typel, O. Riedl, H.H. Wolter, *Nucl. Phys.* **A** in print.
13. C. Fuchs, T. Gaitanos, H.H. Wolter, *Phys. Lett.* **B381** (1996) 23.
C. Fuchs, P. Essler, T. Gaitanos, H.H. Wolter, *Nucl. Phys.* **A626** (1997) 987.
14. L. Sehn, H.H. Wolter, *Nucl. Phys.* **A601** (1996) 473.
15. P. Danielewicz, *Ann. Phys.* **152** (1984) 239, 305.
W. Botermans, R. Malfliet, *Phys. Rep.* **198** (1990) 115.
16. T. Gaitanos, C. Fuchs, H.H. Wolter, Amand Faessler, *Eur. Phys. J.* **A12** (2001)

- 421.
17. A. Andronic et al. (FOPI Collaboration), *Nucl. Phys.* **A661** (1999) 333c.
N. Bastid (FOPI Collaboration), private communication.
 18. P. Danielewicz, *Nucl. Phys.* **A673** (2000) 375.
 19. P. Danielewicz et al., *Phys. Rev. Lett.* **81** (1998) 2438.